npg

ORIGINAL ARTICLE

S-acylation-dependent association of the calcium sensor CBL2 with the vacuolar membrane is essential for proper abscisic acid responses

Oliver Batistič[1], Marion Rehers[1], Amir Akerman[2], Kathrin Schlücking[1], Leonie Steinhorst[1], Shaul Yalovsky[2], Jörg Kudla[1]

[1]Institut für Biologie und Biotechnologie der Pflanzen, Universität Münster, Schlossplatz 4, Münster 48149, Germany; [2]Department of Molecular Biology and Ecology of Plants, Tel Aviv University, Ramat Aviv, Tel Aviv 69978, Israel

Calcineurin B-like (CBL) proteins contribute to decoding calcium signals by interacting with CBL-interacting protein kinases (CIPKs). Currently, there is still very little information about the function and specific targeting mechanisms of CBL proteins that are localized at the vacuolar membrane. In this study, we focus on CBL2, an abundant vacuolar membrane-localized calcium sensor of unknown function from *Arabidopsis thaliana*. We show that vacuolar targeting of CBL2 is specifically brought about by S-acylation of three cysteine residues in its N-terminus and that CBL2 S-acylation and targeting occur by a Brefeldin A-insensitive pathway. Loss of CBL2 function renders plants hypersensitive to the phytohormone abscisic acid (ABA) during seed germination and only fully S-acylated and properly vacuolar-targeted CBL2 proteins can complement this mutant phenotype. These findings define an S-acylation-dependent vacuolar membrane targeting pathway for proteins and uncover a crucial role of vacuolar calcium sensors in ABA responses.

Introduction

Almost all extracellular signals elicit changes in cellular Ca^{2+} concentration. In plants these signals include hormones, light, stress factors and pathogenic or symbiotic elicitors. In addition, physiological processes like guard cell regulation, root hair elongation and pollen-tube growth are accompanied by distinct spatio-temporal changes in Ca^{2+} concentration [1, 2]. The specific signatures of these Ca^{2+} transients can encode information and contribute to the specificity required for efficient stimulus-response coupling. Ca^{2+}-binding proteins translate the information encoded by Ca^{2+} signatures into stimulus-specific cellular responses [1]. Calcineurin B-like (CBL) proteins represent Ca^{2+}-binding proteins which specifically interact with a family of serine-threonine protein kinases designated as CBL-interacting protein kinases (CIPKs) [3, 4]. CBL proteins are closely related to Calcineurin B and to neuronal calcium sensors, including frequenin and recoverin, while CIPKs belong to the superfamily of SNF-like kinases [5, 6]. The genome of the plant *Arabidopsis thaliana* encodes 10 CBLs and 26 CIPK-type kinases [7]. Protein interaction studies revealed a network-like organization of this signaling system in that the selectivity of CBL/CIPK complex formation represents one of the mechanisms generating specificity in signal transmission [8].

Reverse-genetics analyses of individual CBLs and CIPKs have established their important functions in plant mineral nutrition, responses to abiotic stresses and hormones like abscisic acid (ABA) and in modulating ion fluxes [9, 10]. At the plasma membrane CBL1 and CBL9 form complexes with and function in regulating their target CIPK23. Upon activation by CBL1 or CBL9, CIPK23 phosphorylates the Shaker-like K^+ channel

AKT1 and contributes to K$^+$ uptake under limiting K$^+$-supply conditions [11] and to stomata regulation under dehydrating conditions that cause increases in the cellular concentration of the stress responsive phytohormone ABA [12].

Increases in cellular ABA concentration trigger the production of cyclic ADP-ribose and subsequent increases of cytoplasmic Ca^{2+} concentration [13, 14]. These ABA induced Ca^{2+} signatures originate from different sources, including influx from the extracellular space, but also release from internal stores like the central vacuole. Calcium fluxes through the plasma and vacuolar membranes are important for ABA-mediated stomatal closure and are differently regulated depending on specific ABA concentrations [15].

Calcium binding by sensor proteins represents the first level of events for further downstream processing of ABA-induced calcium signals to regulate distinct processes at the plasma membrane and the vacuolar membrane. This requires that defined calcium-binding proteins are specifically targeted to the distinct cellular membranes. Recent work has established that four of the ten CBL calcium sensor proteins from *Arabidopsis* are targeted to the plasma membrane and that another subset of four CBL proteins are specifically localized to the vacuolar membrane [16]. These distinct subcellular localizations suggest that the CBL Ca^{2+} sensors might function as relays of local Ca^{2+} release events from internal and external stores and that the spatial separation of distinct CBL/CIPK complexes contributes to spatial specificity in Ca^{2+} signaling. The specific localization of plasma membrane-localized calcium sensors like CBL1 is brought about by dual lipid modifications through N-myristoylation and S-acylation [17]. However, the mechanisms that govern the vacuolar membrane targeting of CBL proteins or other proteins in general is largely unknown. Moreover, the physiological role of CBL proteins that are specifically targeted to the vacuolar membrane is still enigmatic.

In this work, we focus on characterizing the targeting mechanism and function of the vacuolar calcium sensor CBL2. We report that targeting of CBL2 occurs by S-acylation of three cysteine residues, which are located within the CBL2 N-terminus. This targeting occurs independently of any other lipid modifications such as N-myristoylation or C-prenylation. Moreover, this targeting is not affected in the presence of Brefeldin A, Wortmannin and other inhibitors of vesicle formation. Importantly, a short peptide fragment of the CBL2 N-terminus is sufficient to target the green fluorescent protein (GFP) specifically to the vacuolar membrane. These data uncover a novel targeting mechanism for vacuolar membrane-targeted proteins and reveal remarkable dif-

ferences to the mammalian S-acylation machinery where the Golgi is assumed to represent a possible super-reaction center for peripheral membrane proteins [18, 19]. Moreover, we report that CBL2 plays a crucial role in proper responsiveness to the hormone ABA during early seedling development and provide evidence that S-acylation-dependent vacuolar membrane targeting of CBL2 is absolutely required for this function. Together our data demonstrate the importance of Ca^{2+} sensing at the internal vacuolar Ca^{2+} store for proper hormonal responses and reveal S-acylation-dependent targeting as an important mechanism mediating specific targeting of proteins to the vacuolar membrane.

Results

Targeting of CBL2 to the vacuolar membrane depends on S-acylation

We previously identified the calcium-sensor protein CBL2 from *Arabidopsis* as being specifically targeted to the vacuolar membrane [16]. In order to elucidate the mechanisms responsible for this specific targeting, we examined the membrane-binding properties of CBL2 by biochemical membrane fractionation and solubilization analyses. To this end, CBL2 was fused to an HA tag and transiently expressed in *Nicotiana benthamiana* leaves for sub-cellular protein fractionation analyses in the presence of different chemicals. We determined the influence of EDTA and divalent cations such as calcium and magnesium to address the possibility of a calcium-membrane switch mechanism mediating the vacuolar recruitment of CBL2. Moreover, we applied high concentrations of salt (1 M NaCl) to disrupt the potential electrostatic interactions and the non-ionic detergent Triton X-100 (1%) to disrupt the membrane integrity. These experiments revealed that addition of calcium or EDTA, or incubation with high concentrations of salt did not influence CBL2 membrane binding (Figure 1A). However, solubilization of CBL2 was observed in the presence of Triton, implicating that the membrane-binding of CBL2 occurs by insertion into the lipid layer and suggesting a lipid-dependent anchoring of this protein in the membrane.

We addressed the possibility that CBL2 is S-acylated *in planta* by inhibiting this lipid modification using 2-dibromopalmitate (2-Br). For these analyses CBL2 was fused to GFP and during transient expression in *N. benthamiana* leaves, samples were incubated in 50 μM 2-Br or in a control solution containing 0.05% MeOH. As a control for transmembrane domain-dependent vacuolar membrane-targeted protein, we employed the two-pore K$^+$ channel 1 (TPK1) fused to GFP [20]. Moreover, together with the respective GFP fusion proteins, we co-

expressed the soluble orange/red fluorescence protein (OFP) that decorates the cytoplasm and the nucleus of plant cells [16]. As depicted in Figure 1B, incubation with 2-Br abolished vacuolar membrane targeting of CBL2, which instead accumulated in the cytoplasmic and nuclear compartments. In contrast, vacuolar membrane targeting of the transmembrane domain-containing TPK1 protein was not affected, supporting a specific inhibition of CBL2-membrane attachment. These data strongly suggest that CBL2 targeting to the vacuolar membrane requires the activity of protein S-acyltransferases (PATs) *in planta*.

The N-terminus of CBL2 is required and sufficient to mediate vacuolar membrane targeting in planta

CBL proteins share a rather conserved central-core domain encompassing their four calcium-binding EF hands but harbor specific N-terminal domains that are variable in sequence and length [16]. For plasma membrane-targeted CBL proteins like CBL1, it has been established that this N-terminus is sufficient for providing a target for dual lipid modification by *N*-myristoylation and S-acylation and to dominantly confer plasma membrane association of the fusion proteins [17]. We therefore investigated the importance of the CBL2 N-terminus for
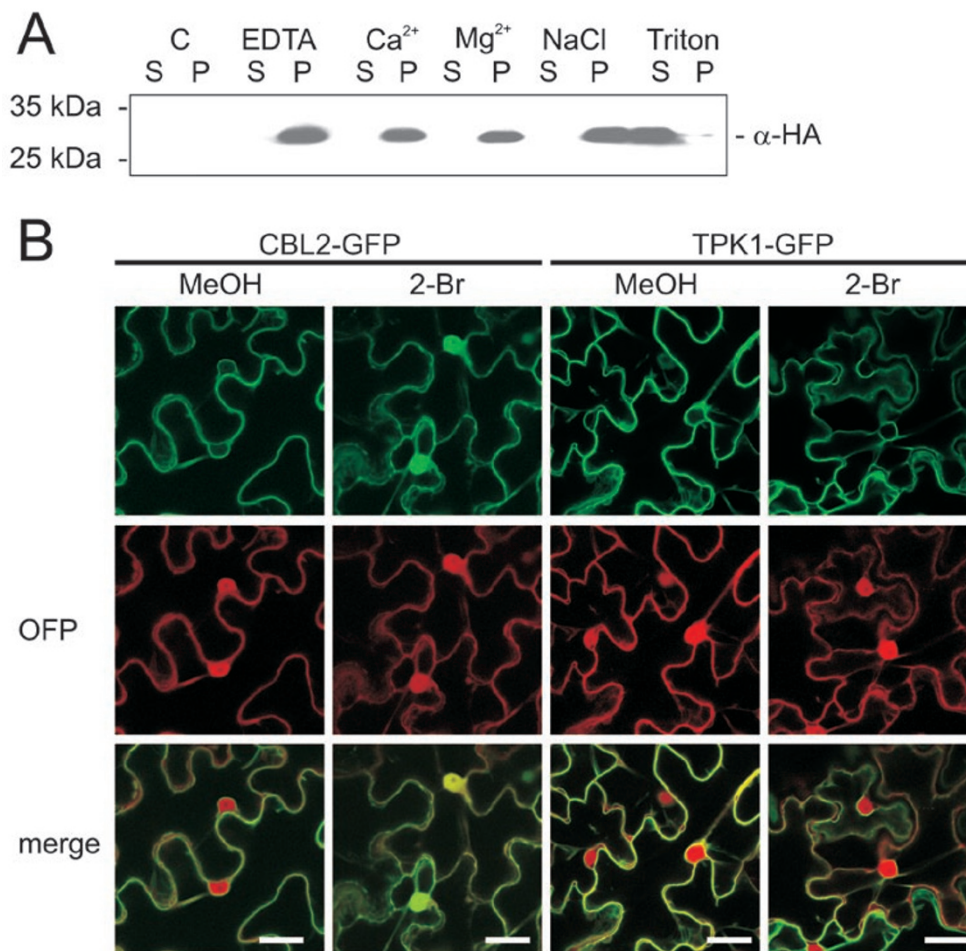

Figure 1 CBL2 is stably associated with a membrane fraction and vacuolar membrane association of CBL2 is abolished by 2-Bromopalmitate. **(A)** To analyze how CBL2 is associated with a membrane fraction, CBL2-HA was transiently expressed in *N. benthamiana* leaves for 2 days. Native proteins were extracted in presence of 10 mM EDTA (EDTA), 10 mM Calcium (Ca^{2+}), 10 mM MgCl$_2$ (Mg^{2+}), 1 M salt (NaCl) or 1% Triton X-100 (Triton) at 4 °C. Extracted proteins were fractionated by a 1 h 100 000× *g* centrifugation step. The soluble (S) and pellet (P) protein fractions were analyzed by western blotting as described in the Materials and Methods section. Mock infiltrated leaves (expressing GFP and extracted with EDTA) were used to prepare a control sample (C). **(B)** CBL2-GFP and the vacuolar protein TPK1-GFP were expressed transiently in *N. benthamiana* leaves for 2 days, together with the soluble cytosolic marker protein OFP. One day after leaf infiltration, samples were taken and incubated in tap water with either 0.05% MeOH and 0.005% Tween (MeOH control) or 50 μM 2-Bromopalmitate and 0.005% Tween (2-Br) and incubated for at least 16 h. Bars represent 20 μm.

its proper targeting by comparatively analyzing the sub-cellular localization of a full-length CBL2-GFP protein and an N-terminally truncated version lacking the first 15 amino acids (CBL2Δn-GFP). In contrast to the full-length CBL2 protein, which targeted the GFP moiety to the vacuolar membrane as expected, deletion of the CBL2 N-terminus in CBL2Δn-GFP diminished the membrane association of the fusion protein and resulted in its accumulation throughout the cytoplasm and the nucleus (Figure 2A). This result identified the CBL2 N-terminus as being required for vacuolar membrane association.

We next examined if the CBL2 N-terminal fragment would be sufficient for efficient vacuolar membrane targeting and sought to determine the minimal structural requirements for this process. We comparatively analyzed the localization of a fusion construct with the first 16 amino acids of CBL2 fused to GFP (CBL2n16-GFP) and a construct that represented a fusion of the first 22 amino acids of CBL2 to GFP (CBL2n22-GFP) in *N. ben-*

Figure 2 The N-terminal CBL2 fragment, harboring three cysteine residues, is sufficient for efficient targeting to the vacuolar membrane. **(A)** The first 15-aa from the CBL2 N-terminus were removed from the protein (CBL2Δn). A GFP fusion protein was transiently expressed in *N. benthamiana* leaves for 2 days, together with a soluble cytosolic OFP marker protein. Bars in the merged pictures represent 20 μm. **(B)** Different fragments of the CBL2 N-terminus harboring either 16-aa (with the first two cysteine residues) or 22-aa (with three cysteine residues) were fused to the N-terminus of GFP. The various GFP fusion proteins were transiently expressed in *N. benthamiana* leaves for 2 days together with the soluble cytosolic marker protein OFP, and microscopically analyzed. Bars in the merged pictures represent 20 μm. **(C)** CBL2n22-GFP does not associate with the plasma membrane. CBL2n22-GFP and the plasma membrane associated CBL1n-OFP marker protein were transiently expressed in *N. benthamiana* leaves for 2 days. Bars represent 10 μm. **(D)** Different fragments of the CBL2 N-terminus harboring either 12-aa (with the first two cysteine residues) or 22-aa (with all three cysteine residues) were fused to the N-terminus of GFP. Wild-type GFP was used as a control. Proteins were transiently expressed in *N. benthamiana* leaves for 2 days. Native proteins were extracted and sub-cellularly fractionated by a 1 h 100 000× *g* centrifugation step. The soluble (S) and pellet (P) protein fractions were analyzed by western blotting as described in the Materials and Methods section. Mock-infiltrated leaves (expressing a HA tagged protein) were used to prepare a control sample (C). **(E)** Membrane association of CBL2n22-GFP is affected by 2-Bromopalmitate. CBL2n22-GFP was transiently expressed in *N. benthamiana* leaves for 2 days together with the soluble cytosolic marker protein OFP. One day after the leaf infiltration, samples were taken from the leaves and incubated in tap water with either 0.05% MeOH and 0.005% Tween (MeOH control) or 50 μM 2-Bromopalmitate and 0.005% Tween (2-Br), incubated for 16 h and microscopically analyzed. Bars represent 20 μm.
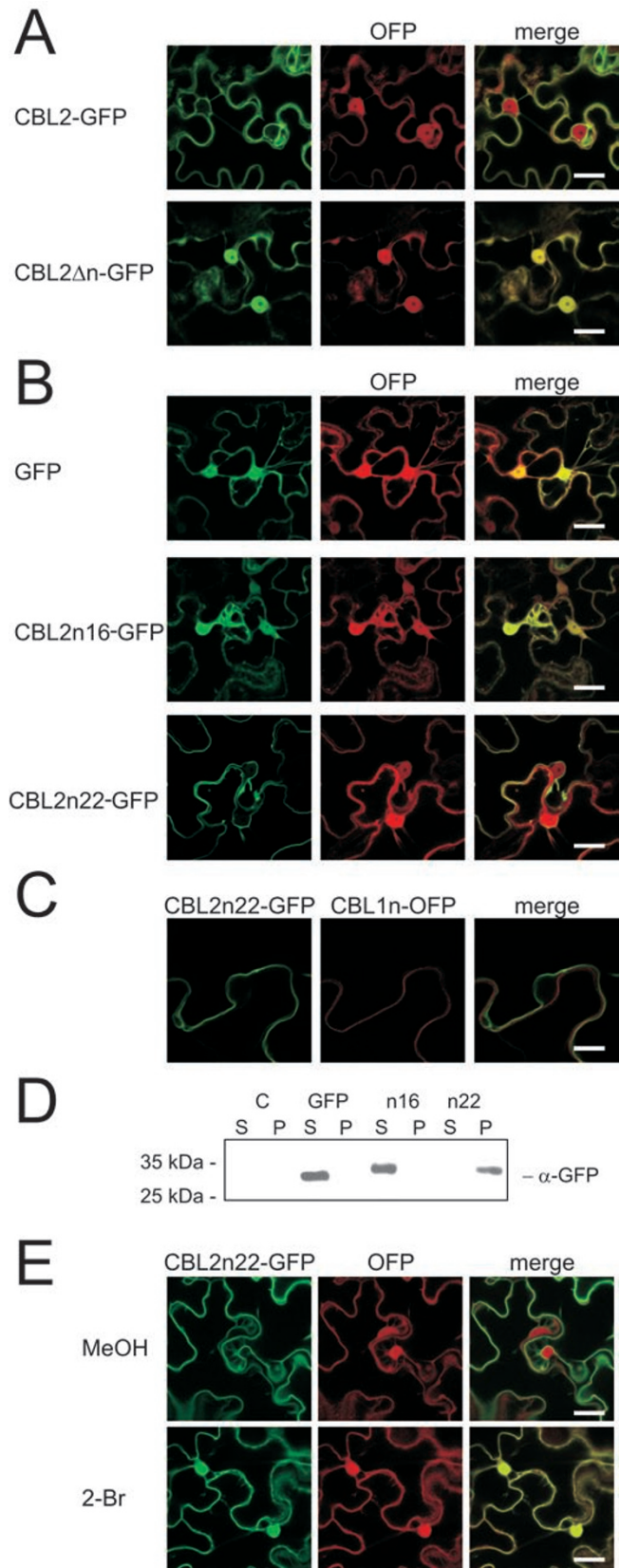
thamiana leaves co-expressing OFP as the cytoplasmic and nuclear marker protein. While CBL2n16-GFP was distributed throughout the cytoplasm and nucleoplasm, accumulation of CBL2n22-GFP appeared to be confined to the vacuolar membrane (Figure 2B). To exclude potential artifacts due to the expression in heterologous species, we also analyzed the localization of the fusion protein in *Arabidopsis thaliana*. A similar pattern was observed when the protein was expressed in *A. thaliana* leaves (Supplementary information, Figure S1). We then investigated if the short 22-aa fragment of CBL2 confers a specific binding to the vacuolar membrane by comparing the localization of CBL2n22-GFP with that of a plasma membrane-targeted OFP protein (PM-OFP). This protein contains the myristoylated-acylated SH4 domain of CBL1, which specifically mediates plasma membrane binding [17]. Co-expression of both proteins clearly revealed distinct localization patterns in which PM-OFP decorated the plasma membrane and CBL2n22-GFP accumulated exclusively at the vacuolar membrane (Figure 2C; and Supplementary information, Figure S2, with line scan). These findings were further corroborated by biochemical-separation analyses that revealed membrane association of CBL2n22-GFP while CBL2n16-GFP and GFP were only detected in soluble fractions after transient expression of these proteins in *N. benthamiana* leaves (Figure 2D). Together, these results indicate that the short 22-aa N-terminal fragment of CBL2 not just confers general membrane association but instead is fully sufficient to mediate specific targeting to the vacuolar membrane. To address if the 22-aa fragment of CBL2n22-GFP mediates vacuolar membrane targeting in an S-acylation-dependent manner, we again applied 2-Br in our localization analyses. As observed for the CBL2 full-length protein, application of 2-Br abolished vacu-

olar membrane targeting of CBL2n22-GFP and resulted in its accumulation throughout the cytoplasm and nucleus (Figure 2E). Together, these results provide strong evidence that the 22-aa N-terminal domain of CBL2 specifically mediates vacuolar targeting via an S-acylation-dependent targeting mechanism.

S-acylation of cysteine residues in the N-terminus directs vacuolar membrane targeting of CBL2

To facilitate the identification of cysteine residues within the N-terminus of CBL2 that could be subject to S-acylation, we used a clustering and scoring strategy (CSS) algorithm that predicts potential S-acylation sites in proteins [21, 22]. This analysis identified two cysteine residues within the CBL2 N-terminus, of which the first cysteine residue at position 4 was predicted to be S-acylated with a high probability score (score: 3.087), while the second cysteine residue at position 12 had a probability score of 0.974. In addition, we performed a BlastP search to identify CBL proteins from different organisms that share a similar extended N-terminal domain with the vacuolar-targeted CBL proteins from *Arabidopsis*. Subsequently, we compared the N-termini of these potentially vacuolar-targeted CBL proteins to determine the conservation of these cysteine residues (Figure 3). While cysteine 4 was absolutely invariant in all sequences analyzed, cysteine 12 appeared to be less conserved. However, we noticed that every CBL protein that lacks cysteine 12 contains a conserved cysteine residue at position 19 in its N-terminus that may provide an alternative S-acylation site (probability score: 3.719 for CBL6). Moreover, we noticed an absolutely conserved cysteine 18 in all CBL proteins analyzed, which was not identified by the CSS S-acylation prediction algorithm using CBL2 (probability score: 0.322), suggesting that
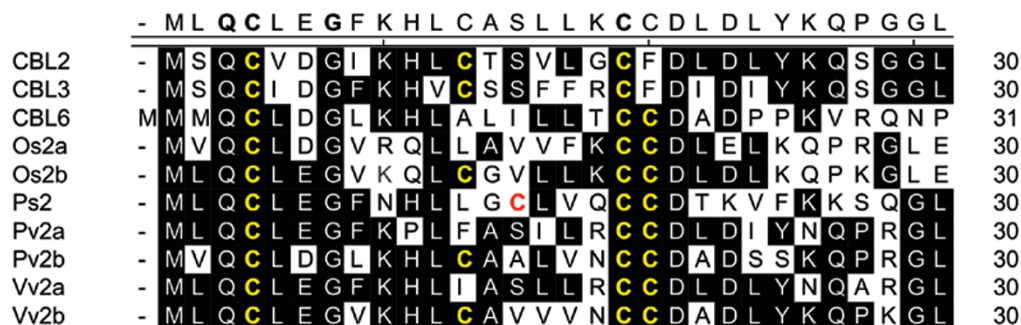

Figure 3 CBL2 and CBL2 related proteins contain several conserved Cys residues within their N-terminal region. The N-terminal regions from CBL2, CBL3 and CBL6 from *Arabidopsis thaliana* and CBL2 related proteins from rice (*Oryza sativa*, Os), spruce (*Picea sitchensis*, Ps), bean (*Phaseolus vulgaris*, Pv), vine (*Vitis vinifera*, Vv) were aligned using the Clustal-W algorithm. Amino acids that are identical in at least two of the compared sequences are highlighted in black. Conserved cysteine residues are decorated in bold yellow.

this cysteine may not represent a substrate of PATs but might be important for target recognition by PATs [21, 23, 24].

To address the individual and combined contribution of these potentially S-acylated cysteine residues to CBL2 vacuolar targeting, we generated a collection of mutated CBL2 proteins in that either individual residues (C4S, C12S, C18S) or multiple amino acids (C12,18S and C4,12,18S) were exchanged and that were either tagged with an HA epitope or fused to GFP. We used sub-cellular fractionation analyses to assess the membrane-binding properties of these different mutant proteins and found that only the CBL2 wt protein was exclusively detected in the membrane fraction, while CBL2C4S, CBL2C18S, CBL2C12,18S and CBL2C4,12,18S were detected in the soluble fraction but not in the insoluble fraction (Figure 4A). In contrast, CBL2C12S was present in both the pellet fraction and to some extent in the soluble fraction. We also investigated the localization of these mutants as GFP fusion proteins in planta. All investigated CBL2 mutant versions, including those with only a single cysteine residue mutated, exhibited diminished vacuolar membrane targeting resulting in cytoplasmic and nucleoplasmic accumulation of the proteins. Only in the case of CBL2C12S, we observed partial binding to the vacuolar membrane (Figure 4B), confirming the results of the fractionation analyses. To exclude that mutations in the N-terminus non-specifically interfere with efficient vacuolar targeting by disturbing the structure of this domain instead of by affecting its S-acylation status, we mutated the conserved glutamine at position 3 to glutamate. This mutation did not affect vacuolar targeting of the CBL2 protein (Supplementary information, Figure S3). Finally, we confirmed the importance of the cysteine residues for the localization of CBL2n22-GFP fusion protein by mutating cysteine 4 to serine (C4S) or exchanging all three cysteine residues to serine (C4,12,18S) (Figure 4C). To further corroborate these findings, the latter protein, together with wild-type GFP and CBL2n22-GFP, was also expressed and analyzed in *A. thaliana* leaves (Supplementary information, Figures S1 and S4). These results demonstrate that in *Arabidopsis* lipid modification of the N-terminus is sufficient and required for correct targeting. Together our results unambiguously establish the critical importance of each of the three N-terminal cysteine residues of CBL2 for effective vacuolar membrane targeting.

We then intended to unequivocally identify the identity of lipid modifications of CBL2. We therefore determined the fatty acyl modification of CBL2 by gas chromatography-mass spectrometry (GC-MS) analysis. To this end, we expressed CBL2-GFP and the triply mutated CBL2C4,12,18S-GFP fusion proteins transiently in *N. benthamiana*. The expression of both proteins was monitored by detecting GFP fluorescence in leaves microscopically. Both proteins were purified from plant-protein extracts (Supplementary information, Figure S5) and the lipid moieties of the protein were removed by hydrogenation and analyzed by GC-MS [25]. This analysis revealed lipid modification of wild-type CBL2 by stearate and palmitate that was not detectable in the CBL2C4,12,18S-GFP protein (Figure 5). In previous work [26], we showed that palmitate (C16 chain) does not accumulate as a result of stearate (C18 chain) breakdown. Therefore, these results indicate that CBL2 is S-acylated *in vivo* by palmitate and stearate. Although our data do not allow to distinguish if there is a difference in the ratio of acylation by either palmitate or stearate between the individual cysteine residues (C4, C12 or C18) or if all the three sites are modified by palmitate or stearate, the complete absence of acylation in the CBL2C4,12,18S-GFP protein excludes S-acylation of any other residues within the CBL2 protein. Therefore, these results unambiguously demonstrate S-acylation of CBL2 *in vivo* and establish the N-terminal domain of this protein as being sufficient for lipid modification and S-acylation-dependent vacuolar membrane targeting *in planta*.

Blockage of vesicle trafficking does not affect S-acylation and vacuolar membrane targeting of CBL2

In mammalian cells, the Golgi compartment has recently emerged as the central reaction center for the cellular S-acylation machinery [18]. Here this organelle provides directionality in the acylation cycle by allowing locally S-acylated proteins to enter the secretory pathway from where they are targeted to peripheral membranes. In contrast, our previous work has established a Golgi-independent pathway for plasma membrane targeting of the CBL1 protein that depends on lipid modification by myristoylation and S-acylation in plant cells [17]. Remarkably, treatment with Brefeldin-A (BFA) that interferes with post-ER transport processes or co-expression of the dominant-negative Sar1 mutant did not impede CBL1 trafficking or S-acylation. We therefore further investigated the vacuolar membrane targeting pathway of the S-acylated CBL2 protein.

We compared the localization of CBL2-GFP in transiently transformed *N. benthamiana* leaves that were treated with 50 µM BFA, 20 µM Wortmannin or with 0.05% DMSO as a solvent control. In addition, we co-expressed a dominant-negative mutant version of Sar1 (H74L) to block export from the ER [27]. As a control for the efficiency of the drug treatments and of the
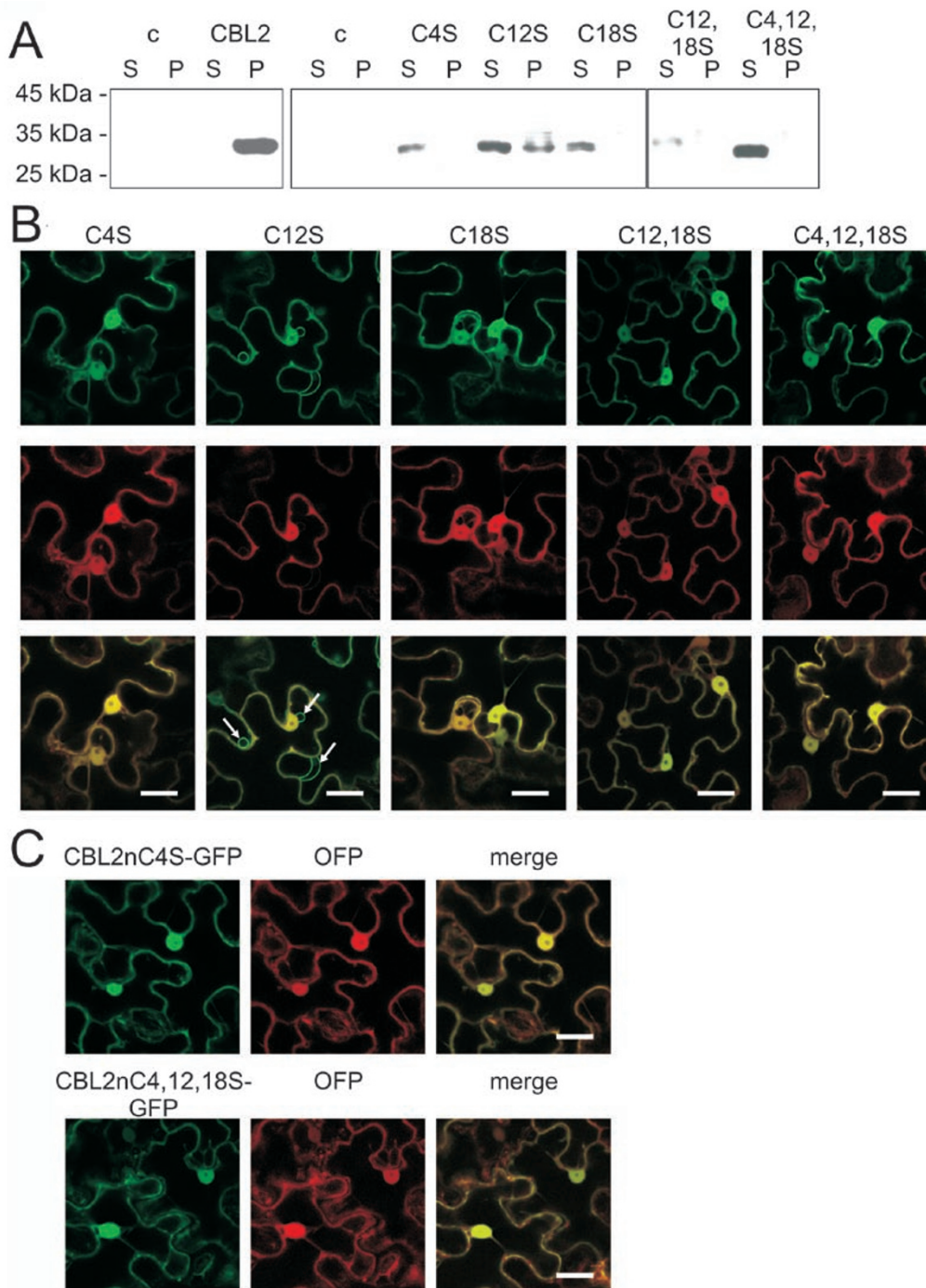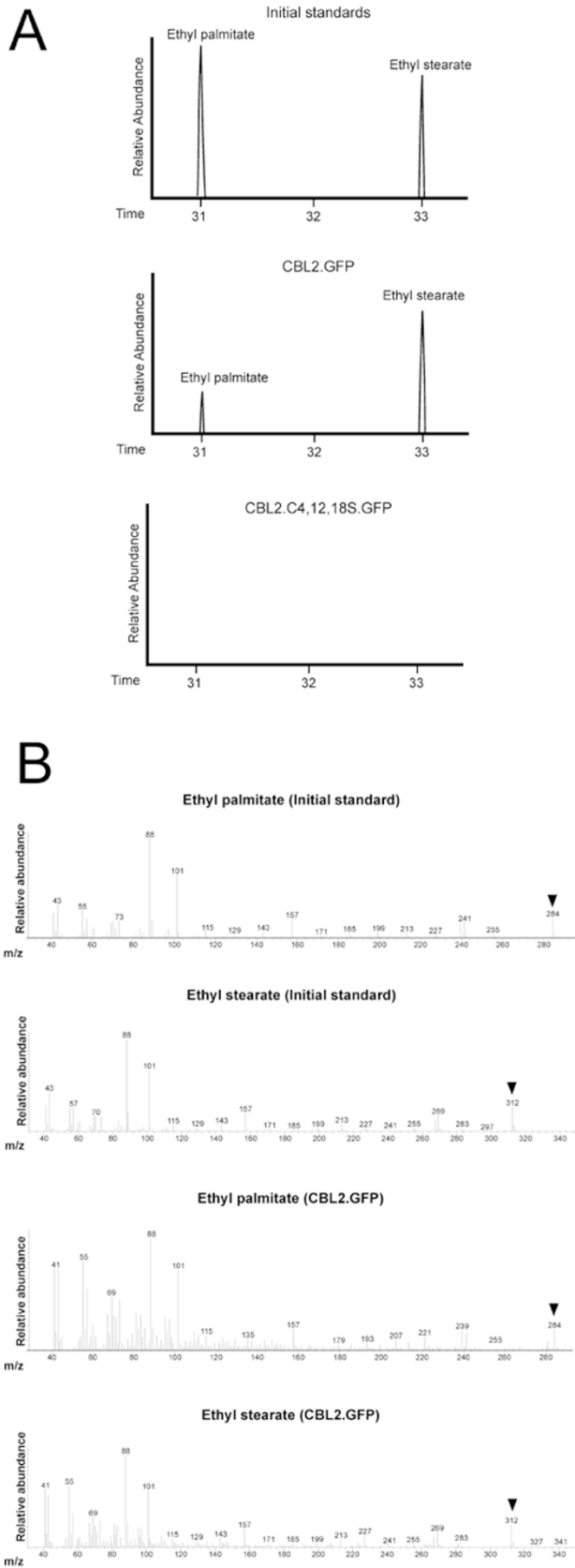
Figure 4 S-acylation of three cysteins in the N-terminus directs vacuolar membrane targeting of CBL2. **(A)** Different versions of CBL2, which contain either single cysteine to serine exchanges (C4S, C12S, C18S), two cysteine to serine exchanges (C12, 18S), or three cysteine to serine exchanges (C4,12,18S) were generated. HA tagged versions were transiently expressed in *N. benthamiana* leaves for 2 days. Native proteins were extracted and sub-cellularly fractionated by a 1 h 100 000× *g* centrifugation step. The soluble (S) and pellet (P) protein fractions were analyzed by western blotting as described in the Materials and Methods section. Mock infiltrated leaves (expressing a GFP protein) were used to prepare a control sample (C). **(B)** Different versions of CBL2, which contain either single cysteine to serine exchanges (C4S, C12S, C18S), two cysteine to serine exchanges (C12,18S), or three cysteine to serine exchanges (C4,12,18S) were fused with GFP. Proteins were transiently expressed for 2 days in *N. benthamiana* leaves together with a soluble cytosolic OFP marker protein, and analyzed microscopically. Bars in the merged pictures represent 20 μm. **(C)** Different mutated versions of the CBL2 N-terminal peptide fused to GFP (CBL2nC4S and CBL2nC4,12,18S) transiently expressed in *N. benthamiana* leaves, together with the cytosolic OFP control protein. Epidermal cells were microscopically analyzed. Bars in the merged pictures represent 20 μm.

A
Initial standards

Ethyl palmitate

Ethyl stearate

Relative Abundance

Time 31 32 33

CBL2.GFP

Ethyl stearate

Ethyl palmitate

Relative Abundance

Time 31 32 33

CBL2.C4,12,18S.GFP

Relative Abundance

Time 31 32 33

B
Ethyl palmitate (Initial standard)

Relative abundance

m/z

Ethyl stearate (Initial standard)

Relative abundance

m/z

Ethyl palmitate (CBL2.GFP)

Relative abundance

m/z

Ethyl stearate (CBL2.GFP)

Relative abundance

m/z

Sar1H74L co-expression, we analyzed the localization of OFP-TM23, a modified secreted version of OFP containing a transmembrane domain, which results in plasma membrane targeting [28]. While the localization of OFP-TM23 was strongly affected by BFA, Wortmannin or by Sar1H74L co-expression, leading to relocation of fluorescence from the PM to internal compartments, the vacuolar membrane targeting of CBL2-GFP was not inhibited (Figure 6). Consequently, these data establish that vacuolar membrane targeting of CBL2 relies on a BFA- and Wortmannin-insensitive pathway and does not require the export from the ER by COPII vesicles. Moreover, these findings suggest that acylation of CBL2 is not impaired by BFA or Wortmannin, and support the conclusion that CBL2 is directed to the vacuolar membrane via a novel targeting mechanism.

CBL2 function and vacuolar targeting are essential for appropriate ABA responses

While cellular targeting mechanisms and physiological functions have been established for several plasma membrane-localized CBL proteins, there is still very little information about CBL proteins that are localized at the vacuolar membrane. We therefore isolated a homozygous CBL2 T-DNA insertion line (SALK_115461) that was obtained from the Salk Institute Genomic Analysis Laboratory T-DNA collection. Sequence analyses of the PCR products amplified with primer combinations specific for both flanking regions of the T-DNA localized the T-DNA insertion between the 5th and 6th exon, 843 nucleotides downstream of the ATG initiator codon (Supplementary information, Figure S6A). The T-DNA insertion event turned out to be accompanied by a deletion of 15 bp of the genomic DNA. Expression of functional *CBL2* mRNA was reduced to undetectable levels by the T-DNA insertion (Supplementary information, Figure S6B).

Figure 5 CBL2 is modified by stearate and palmitate. CBL2-GFP and a mutated version of CBL2 harboring the triple cysteine to serine exchanges (C4,12,18S) were transiently expressed in *N. benthamiana* leaves. Native proteins were extracted from the leaf material and GFP-tagged proteins were enriched by differential ammonium sulfate precipitations and ion-exchange chromatography. Lipid groups were removed by hydrogenation and analyzed by GC coupled MS analyses. **(A)** GC retention and identification of standard ethyl palmitate (after 32 min) and ethyl stearate (after 34.3 min) derivatives (bottom chromatogram), and of the hydrogenated lipids removed from CBL2-GFP and CBL2C4,12,18S-GFP. **(B)** MS chromatograms of the ethyl palmitate and ethyl stearate standards (top panels) and of ethyl palmitate and ethyl stearate released from CBL2-GFP (bottom panels).

These data suggest that the identified T-DNA insertion line harbors a *cbl2* loss-of-function allele designated here as *cbl2-1*. Despite the virtually complete absence of the *CBL2* transcript, the *cbl2-1* mutant plants did not exhibit an obvious phenotype under normal growth conditions.

Our earlier mutant analyses of the plasma membrane-localized calcium sensor CBL9 had established that this protein mediates ABA-dependent stress responses [29]. Ca^{2+} signals emanating from the intracellular vacuolar Ca^{2+} store are also known to contribute to ABA signaling
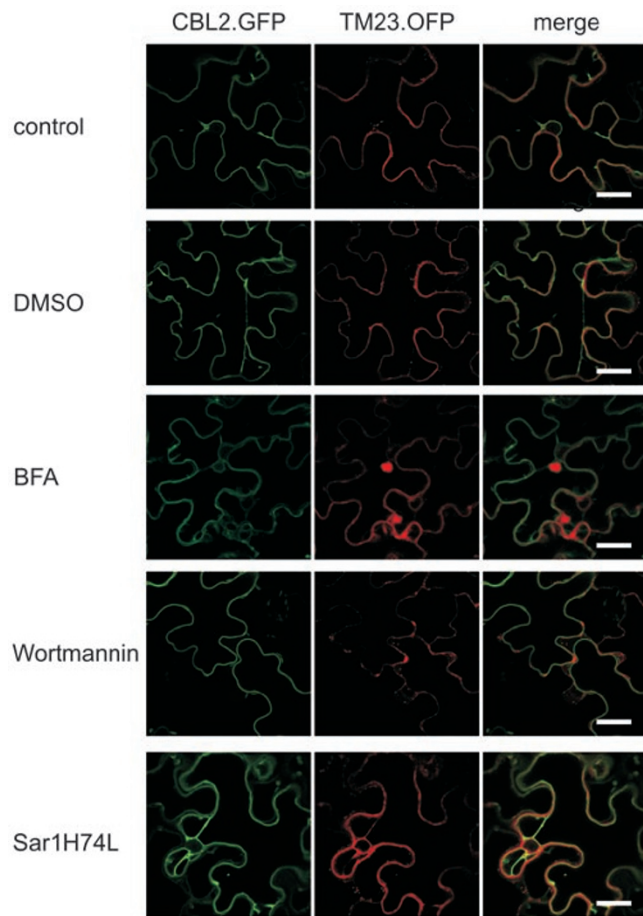

Figure 6 Brefeldin-A, Wortmannin or Sar1H74L co-expression does not affect S-acylation and vacuolar membrane targeting of CBL2. CBL2-GFP and the plasma membrane-targeted OFP-TM23 protein were transiently expressed in *N. benthamiana* leaves (control). Either DMSO (solvent control), 50 μM BFA or 20 μm Wortmannin were applied to the infiltrated leaves and localization of proteins were examined in epidermal cells after 16 h of incubation. In addition, a dominant negative version of Sar1 (Sar1H74L) was co-expressed. In presence of BFA or Wortmannin, OFP-TM23 accumulates in intracellular compartments, while Sar1H74L co-expression blocks the export from the ER. In contrast, localization of CBL2-GFP is not affected. Bars in the merged pictures represent 20 μm.

by largely unknown mechanisms [10]. We therefore were especially interested in testing the possible involvement of CBL2 in ABA-mediated stress responses. However, CBL2 forms a gene pair with CBL3. The two proteins are 92% identical [30] and share similar expression patterns [31], suggesting that they may exhibit overlapping functions. Nevertheless, we attempted to identify discernable phenotypes of a *cbl2* mutant. We did not observe convincing differences in the ABA-dependent regulation of stomatal closure or in seedling-survival assays (Supplementary information, Figure S7A and S7B). Nevertheless, we additionally comparatively determined the germination rates of Col-0 wild type and *cbl2-1* seeds on media with or without supplementation of ABA. As depicted in Figure 7, application of 5 μM ABA dramatically reduced the germination rate of *cbl2-1* seeds when compared with wild type.

We next employed this ABA sensitive phenotype of the *cbl2-1* mutant to investigate the relevance of S-acylation for the functionality of this calcium sensor protein. To this end, we transformed cDNAs encoding the CBL2 wild-type sequence as well as mutant versions of CBL2 (CBL2C4S and CBL2C4,12,18S) under the control of the native CBL2 promoter into the *cbl2-1* mutant. As specificity control, a chimerical protein comprising the CBL2 N-terminus fused to the closely related calcium sensor CBL1 (CBL2nCBL1) that interacts with similar CIPKs as CBL2 [17] and which is thereby targeted to the vacuole (Supplementary information, Figure S8) was introduced into the cbl2-1 mutant background. For each construct, three independent homozygous F2 lines were generated and initially analyzed. The expression levels of the transgenes were verified by RT-PCR (Supplementary information, Figure S6B). Germination rates of the seeds were scored after 5 days of exposure to ABA. All analyzed transgenic lines without wild-type CBL2 exhibited a similar phenotype. Therefore, detailed analyses were performed in triplicate with all the three independent lines and one representative experiment is presented in Figure 7. In these analyses only plants complemented with the CBL2 wt protein exhibited an ABA response similar to the wild-type plants (36.3% ± 2% germinated seeds and 46.3 % ± 3.3%, respectively; Student's *t*-test *P* value = 0.06) (Figure 7), while all other modified CBL2 proteins did not significantly enhance the germination rate when compared to the *cbl2-1* mutant line (*cbl2-1* 16.7% ± 0.9%; *2-1*/CBL2nCBL1 13% ± 1.7%; *2-1*/CBL2C4S 18.3% ± 3.3%; *2-1*/CBL2C4,12,18S 17.3% ± 1.7%; for *P* values see Supplementary information, Table S2). These results demonstrate that S-acylation of CBL2 is essential for its function and that this protein has to be efficiently targeted to the vacuolar membrane to ensure
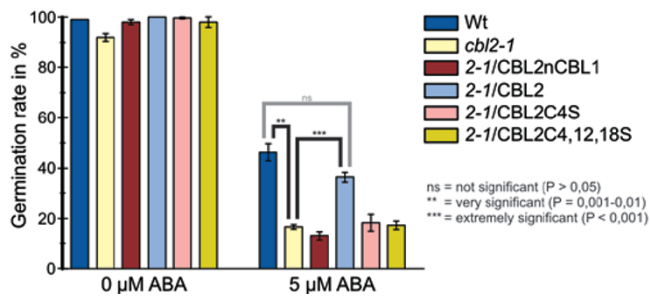
Figure 7 CBL2 function and S-acylation-dependent vacuolar targeting are essential for ABA response. Statistical analysis of the germination rates on control plates (0 μM) and on plates supplemented with 5 μM ABA from wild-type plants (Wt), *cbl2-1* knock-out plants (*cbl2-1*), and *cbl2-1* knock-out plants complemented with different CBL2 versions (CBL2 N-terminus fused to CBL1, *2-1*/CBL2nGFP; CBL2 wt version, *2-1*/CBL2; CBL2 C4S exchange, *2-1*/CBL2C4S and CBL2 with C4,12,18S triple exchange, *2-1*/CBL2C4,12,18S). For each of the complemented *cbl2-1* knock-out mutants, three independent lines (100 seeds each independent line) were analyzed in triplicate. Bars represent mean value of germination rate in % after 5 days of incubation, and error bars represent the standard error. Significance was tested using Student's *t*-test.

proper responses to ABA. Moreover, these finding also indicate that the lipid groups of the CBL2 N-terminus *per se* are not the functional determinants for proper ABA responses, as the related CBL1 protein fused with the CBL2 N-terminus can not substitute for CBL2 function.

Discussion

In this study, we characterized the mechanisms by which CBL2, a ubiquitously expressed member of the CBL family of Ca^{2+} sensors, is targeted to the vacuolar membrane in plant cells. Our results show that its targeting relies on lipid modification by S-acylation and that an N-terminal domain of 22 amino acids is required and sufficient to bring about this specific subcellular localization. Inhibition of S-acylation by application of the inhibitor 2-Br results in accumulation of CBL2 in the cytosolic and nuclear compartments but not in the Golgi or TGN suggesting a direct cytoplasm to vacuolar membrane targeting process for this protein.

We subsequently determined the fatty acyl modification of CBL2 by GC-MS analysis. These experiments unequivocally established the modification of this protein by palmitic and stearic acids. A similar dual fatty-acyl modification was previously reported for the plasma membrane-targeted proteins Rho-related GTPase ROP6

and the Ca^{2+} sensor CBL1 from *Arabidopsis* [17, 26]. It is therefore tempting to speculate that dual lipidation by palmitic and stearic acids represents a general enzymatic feature of plant PATs. Within the 22-aa domain of CBL2, we identified three cysteine residues as potential substrates for S-acylation and in our GC-MS analyses we observed that mutation of all the three amino acids completely abolished CBL2 S-acylation.

To clarify the individual and combined contribution of these cysteine residues to the S-acylation and targeting of CBL2, we investigated mutated versions of this protein in which either single C4S, C12S and C18S exchanges or combinations of these mutations were analyzed by biochemical fractionation and microscopic localization analyses. Consistently, in both experimental approaches, we observed that mutation of even a single cysteine already impaired membrane association and targeting to the vacuolar membrane. Remarkably, single C4S and C18S exchanges completely abolished membrane association in our biochemical fractionation studies and resulted in cytoplasmic and nuclear accumulation of the respective GFP fusion proteins in *N. benthamiana* leaves. These results identify both cysteines as being absolutely required for CBL2 membrane recruitment and proper vacuolar membrane targeting. Importantly, an exchange of the third amino acid adjacent to cysteine 4 from glutamine to glutamate, (CBL2Q3E) that imparts a reduction of the negative charge of the N-terminal CBL2 domain, did not have any effect on membrane association or vacuolar targeting of this protein. This makes non-specific effects of the C4S or C18S mutations on the structure or charge of the N-terminal CBL2 domain as a cause for the abolished vacuolar membrane targeting rather unlikely. This conclusion is further supported by our inhibitor experiments with 2-Br, which affects S-acylation but not the structure of CBL2. In contrast to the C4S and C18S exchanges, the C12S mutant version of CBL2 was detected in both the soluble and the membrane fractions in our biochemical analyses. Consistently, the CBL2C12S-GFP fusion protein accumulated not only in the cytosol and nucleus but also to some extent at the vacuolar membrane. This finding supports the notion that the cysteine 12 residue is less critical for primary vacuolar membrane recruitment of CBL2 but might be important for the stabilization of membrane association upon membrane attachment.

So far the physiological function of members of the CBL Ca^{2+} sensor family that are exclusively localized at the vacuolar membrane has not been elucidated. In this study, we have isolated a loss-of-function mutant of CBL2 and provided evidence that this Ca^{2+} sensor functions in regulating signaling responses to the phytohormone ABA. Previous work has established that ABA

signaling triggers subsequent Ca^{2+} releases into the cytoplasm from external stores through the plasma membrane and from the internal vacuolar store through the vacuolar membrane [15]. Our work identifies CBL2 as the first Ca^{2+} sensor that likely contributes to decoding ABA-induced Ca^{2+} signatures emanating from the vacuole.

CBL proteins have been found to exhibit overlapping functions, as for example, the plasma membrane-localized CBL1 and CBL9 function together in the activation of the K$^+$ channel AKT1 [11, 12]. In this regard, a similar scenario is very likely for the two closely related tonoplast calcium sensors CBL2 and CBL3. Nevertheless, we could employ the ABA-sensitive phenotype of the *cbl2* loss-of-function mutant in a complementation approach to investigate the importance of S-acylation for CBL2 function. Our findings that only the fully S-acylatable CBL2 can restore wild-type ABA responsiveness and that single mutations of S-acylated cysteine residues already interfere with CBL2 function in ABA responses establish the importance of this lipid modification for proper CBL2 function. Since these single cysteine to serine substitutions also impede vacuolar targeting of this Ca^{2+} sensor, these findings also underscore the significance of precise attachment to the vacuolar membrane for appropriate Ca^{2+} signaling in response to ABA. Also of interest is our finding that expression of the CBL2nCBL1 chimera in the *cbl2* mutant did not complement the ABA-sensitive phenotype. Several studies have shown that both Ca^{2+} sensors interact with an overlapping set of CIPK target kinases *in planta*, including, for example CIPK1 that is involved in ABA response [16, 17, 32]. Exchange of the native N-terminus of CBL1 by the N-terminus of CBL2 redirects this fusion protein to the vacuolar membrane, where CBL2 usually exerts its function. The inability of the CBL2nCBL1 fusion protein to compensate the loss of CBL2 function indicates that correct localization and the ability to interact with the same CIPKs are not sufficient to determine the functional specificity of this Ca^{2+} sensor.

Recent work has identified efficient S-acylation of proteins only at the Golgi compartment in mammalian cells [18]. Moreover, S-acylated peripheral membrane proteins such as Fyn, R-Ras and Rap2C all accumulate at the Golgi when vesicle trafficking is blocked [18]. In addition, lysosomal targeting of the mammalian Ca^{2+} sensor synaptotagmin VII requires S-acylation-dependent association with the tetraspanin CD63 at the Golgi [33]. Together, these findings support the conclusion that the Golgi and potentially TGN compartments represent a specialized reaction center for all the S-acylated proteins in mammalian cells [19]. Application of BFA blocks the transport or the S-acylation of peripheral membrane

proteins such as N-Ras and H-Ras or SNAP-25 [34]. As BFA inhibits vesicle transport between ER and the Golgi, negative effects of BFA treatment on protein sorting or S-acylation reflect an involvement of the Golgi in these processes [35]. Wortmannin inhibits phosphatidyl inositol-kinases, thereby also blocks sorting to the vacuole in plant cells [36, 37]. Moreover, expression of a dominant negative version of the Sar1 protein (H74L) inhibits trafficking of vacuolar proteins by efficiently inhibiting COPII vesicle trafficking from the ER [27, 38]. Here we used the application of these three inhibitors that affect distinct steps of trafficking to elucidate the mechanisms of CBL2-GFP trafficking in plant cells. Surprisingly, neither treatment with BFA or Wortmannin, nor overexpression of Sar1H74L impeded vacuolar membrane recruitment or S-acylation of CBL2. These results point to an S-acylation mechanism and cellular targeting process of CBL2 that are different from the S-acylation machinery in mammalian cells. Based on these findings and the cytoplasmic accumulation of CBL2 after application of 2-Br, we hypothesize that recruitment of CBL2 to the vacuolar membrane occurs by a direct cytoplasm to vacuolar membrane switch that may involve specific interaction with a PAT that resides in this membrane. While in mammalian cells none of the 23 different PATs appears to be localized to the lysosomal compartment [39], Pfa3p, one of the 7 PATs encoded in the yeast genome, has been identified as being localized in the vacuolar membrane [40], where this enzyme S-acylates the armadillo repeat protein Vac8p that is essential for vacuole fusion [40-42]. Similar to the situation in yeast at least one of the 23 PATs encoded in the genome of the plant *Arabidopsis thaliana* seems to be localized to the vacuolar membrane [43]. Thus, it appears conceivable that there may be important differences in the S-acylation pathways of mammalian species that contrast the mechanisms underlying S-acylation in yeast and plants. These differences appear not to be restricted to the occurrence of S-acylation at the vacuolar membrane. While in mammalian cells S-acylation of peripheral membrane proteins occurs at the Golgi, in yeast the Ras PAT Erf2 is localized at the ER [44]. Similarly, in plants, the Ca^{2+} sensor CBL1 reaches the peripheral membrane via a two-step lipid-modification process that does not involve the Golgi. Instead, myristoylation of CBL1 targets this protein to the ER where CBL1 undergoes S-acylation that confers plasma membrane targeting of this protein [17].

Despite the limited information that is currently available about the S-acylation processes at the vacuolar membrane in yeast and plants, several differences between the mechanisms in these species are already emerging. Vacuolar targeting of Vac8p from yeast is

brought about by dual lipid modifications through myristoylation and S-acylation and myristoylation has been shown to be required for efficient S-acylation [40, 42, 45]. While S-acylation is required for proper Vac8p function in vacuole fusion it appears to be dispensable for vacuolar targeting. In contrast, vacuolar membrane targeting of CBL2 is exclusively dependent on S-acylation thereby suggesting differences in the enzymatic properties of the vacuolar PATs in yeast and plants. Moreover, there appear to be differences in the interaction and specificity determinants of yeast and plant PATs with their vacuolar substrates. S-acylation of yeast Vac8p by Pfa3p involves a two-step reaction mechanism including initial binding of Pfa3p to the myristoylated Vac8p substrate and subsequent interaction of the DHHC domain [45]. Interestingly, while full-length Vac8p was efficiently and exclusively targeted to the vacuolar membrane as a GFP fusion protein in yeast, an N-terminal fragment of Vac8p fused to GFP resulted in binding to the vacuolar membrane as well as to the plasma membrane. For Vac8p the armadillo repeat 11 was suggested to be important for binding to Pfa3 thereby mediating specific targeting to the vacuolar membrane [42]. In contrast, in our study reported here, we identified an N-terminal fragment of 22 amino acids of CBL2 as being fully sufficient to specifically mediate vacuolar targeting of GFP fusion proteins and our mutational analysis of the cysteine residues in this domain further supported the S-acylation dependence of this process. Moreover, in our previous work we identified an N-terminal 12-aa fragment of the calcium sensor CBL1 as being sufficient to bring about dual lipid modifications by myristoylation and S-acylation and to confer plasma membrane targeting of several fusion proteins [17]. These observations suggest that in contrast to the situation in yeast (and mammalian cells) plant PATs may exhibit a rather specific recognition and interaction mechanism. Overall, the results of this study suggest that the S-acylation machinery in different organisms appears to be more diverse and complex than currently appreciated and uncover the general importance of the cellular S-acylation machinery for generating spatial specificity in decoding Ca^{2+} signals.

Material and Methods

General methods, plant material and cultivation, complementation of the cbl2 mutant and phenotypical assays

Molecular-biology methods were performed according to standard procedures [46]. A list of primers used for the respective constructs, details of plasmid generation and a description of the mutant complementation are provided as Supplementary information, Table S1. *Arabidopsis thaliana* cv. Col-0 plants and *Nicotiana benthamiana* plants were cultivated as described previously [17].

The knockout status of the *cbl2* mutant line was experimentally verified as described previously for CIPK1 [32]. Homozygous T3 complementation lines were analyzed in phenotypical assays that were performed on 0.8% agar and ½ Murashige and Skoog's media, and, if indicated, supplemented with 5 μM ABA (from a 5 mM stock, dissolved in 70% EtOH). Plant seeds were placed on the respective media, placed for two days at 4 °C for stratification and after cultivation for 5 days, the number of seedlings which developed green cotyledons was counted.

Leaf infiltration, protein isolation, membrane fractionation and fluorescence microscopy

For transient *in planta* protein expression, leaves were infiltrated with the *A. tumefaciens* strain GV3101 pMP90, which was transformed with the respective plasmids by electroporation [47]. For leaf infiltration in *N. bethamiana*, *A. tumefaciens* were prepared as described previously [47]. Transient protein expression in *Arabidopsis thaliana* was performed as described by Kim *et al.* [48]. Leaf samples were harvested 2 days after infiltration (4 days with *Arabidopsis*) and immediately frozen in liquid nitrogen or analyzed microscopically. A detailed description of biochemical fractionation conditions is provided as Supplementary information, Data S1.

Fluorescence microscopy was performed as described previously [16, 17]. Fluorescence microscopy was performed with an inverted microscope (Leica DMIRE2) equipped with the Leica TCS SP2 laser-scanning device (Leica Microsystems). Detection of fluorescence was performed as follows: GFP, excitation at 488 nm (Ar/Kr laser), scanning at 500 to 535 nm; yellow fluorescent protein (bimolecular fluorescence complementation), excitation at 514 nm (Ar/Kr laser), scanning at 525 to 600 nm; OFP, excitation at 543 nm (He/Ne laser), scanning at 565 to 595 nm. All images were acquired using a 63× /1.20 water-immersion objective (HCX PL Apo CS) from Leica. All laser-scanning confocal micrographs presented in this study are single optical sections of the middle position of epidermal cells. All images were acquired with an 8 bit, 1 024 × 1 024 pixel resolution and processed using the Leica Imaging software.

In vivo determination of CBL2 lipid modification, 2-Bromopalmitate and inhibitor treatments

Wild-type CBL2 and CBL2C4,12,18S were expressed in *N. benthamiana* and extracted as described in Batistič *et al.* [17]. Brefeldin A treatments and incubation with 2-Bromopalmitate were performed as described previously [16, 17]. Wortmannin (DMSO stock solution) was applied at a concentration of 20 μM. The application of the dominant negative version of the trafficking inhibitor Sar1 (H74L) was described previously [16]. Protein purification was performed from total protein extracts by differential ammonium sulfate precipitations and subsequent ion-exchange chromatography as described in detail in the Supplementary information, Data S1. Cleavage of acyl groups was performed as described previously and in the Supplementary information, Data S1 [25, 26]. GC-MS analyses were performed with an Agilent Technologies GC/MSD system as described in detail in Batistič *et al.* [17].

Accession numbers

Sequence data from this article can be found in the Arabidopsis

Genome Initiative database or in the EMBL/GenBank data libraries under the following accession numbers: *CBL2*, At5g55990; *CBL3*, At4g26570; *CBL6*, At4g16350; *TPK1*, At5g55630; *Oryza sativa CBL2a*, NP_001067190; *Oryza sativa CBL2b*, NP_001050704; *Picea sitchensis CBL2*, ABK22758; *Phaseolus vulgaris CBL2a*, BAG06679; *Phaseolus vulgaris CBL2b*, BAG06680; *Vitis vinifera CBL2a*, CAN72862; *Vitis vinifera CBL2b*, CAN62487.

Acknowledgments

References

1 Dodd AN, Kudla J, Sanders D. The language of calcium signaling. *Annu Rev Plant Biol* 2010; **61**:593-620.

2 Sanders D, Pelloux J, Brownlee C, Harper JF. Calcium at the crossroads of signaling. *Plant Cell* 2002; **14Suppl**:S401-S417.

3 Kudla J, Xu Q, Harter K, Gruissem W, Luan S. Genes for calcineurin B-like proteins in *Arabidopsis* are differentially regulated by stress signals. *Proc Natl Acad Sci USA* 1999; **96**:4718-4723.

4 Shi J, Kim KN, Ritz O, *et al.* Novel protein kinases associated with calcineurin B-like calcium sensors in *Arabidopsis*. *Plant Cell* 1999; **11**:2393-2405.

5 Batistič O, Kudla J. Integration and channeling of calcium signaling through the CBL calcium sensor/CIPK protein kinase network. *Planta* 2004; **219**:915-924.

6 Hrabak EM, Chan CW, Gribskov M, *et al.* The *Arabidopsis* CDPK-SnRK superfamily of protein kinases. *Plant Physiol* 2003; **132**:666-680.

7 Weinl S, Kudla J. The CBL-CIPK Ca$^{(2+)}$-decoding signaling network: function and perspectives. *New Phytol* 2009; **184**:517-528.

8 Batistič O, Kudla J. Plant calcineurin B-like proteins and their interacting protein kinases. *Biochim Biophys Acta* 2009; **1793**:985-992.

9 Hedrich R, Kudla J. Calcium signaling networks channel plant K$^+$ uptake. *Cell* 2006; **125**:1221-1223.

10 Kudla J, Batistič O, Hashimoto K. Calcium signals: the lead currency of plant information processing. *Plant Cell* 2010; **22**:541-563.

11 Xu J, Li HD, Chen LQ, *et al.* A protein kinase, interacting with two calcineurin B-like proteins, regulates K$^+$ transporter AKT1 in *Arabidopsis*. *Cell* 2006; **125**:1347-1360.

12 Cheong YH, Pandey GK, Grant JJ, *et al.* Two calcineurin B-like calcium sensors, interacting with protein kinase CIPK23, regulate leaf transpiration and root potassium uptake in *Arabidopsis*. *Plant J* 2007; **52**:223-239.

13 Leckie CP, McAinsh MR, Allen GJ, Sanders D, Hetherington AM. Abscisic acid-induced stomatal closure mediated by cyclic ADP-ribose. *Proc Natl Acad Sci USA* 1998; **95**:15837-15842.

14 Wu Y, Kuzma J, Marechal E, *et al.* Abscisic acid signaling through cyclic ADP-ribose in plants. *Science* 1997; **278**:2126-2130.

15 MacRobbie EA. ABA activates multiple Ca$^{(2+)}$ fluxes in stomatal guard cells, triggering vacuolar K$^{(+)}$(Rb$^{(+)}$) release. *Proc Natl Acad Sci USA* 2000; **97**:12361-12368.

16 Batistič O, Waadt R, Steinhorst L, Held K, Kudla J. CBL-mediated targeting of CIPKs facilitates the decoding of calcium signals emanating from distinct cellular stores. *Plant J* 2010; **61**:211-222.

17 Batistič O, Sorek N, Schultke S, Yalovsky S, Kudla J. Dual fatty acyl modification determines the localization and plasma membrane targeting of CBL/CIPK Ca^{2+} signaling complexes in *Arabidopsis*. *Plant Cell* 2008; **20**:1346-1362.

18 Rocks O, Gerauer M, Vartak N, *et al.* The palmitoylation machinery is a spatially organizing system for peripheral membrane proteins. *Cell* 2010; **141**:458-471.

19 Salaun C, Greaves J, Chamberlain LH. The intracellular dynamic of protein palmitoylation. *J Cell Biol* 2010; **191**:1229-1238.

20 Czempinski K, Frachisse JM, Maurel C, Barbier-Brygoo H, Mueller-Roeber B. Vacuolar membrane localization of the *Arabidopsis*, 'two-pore' K$^+$ channel KCO1. *Plant J* 2002; **29**:809-820.

21 Planey SL, Zacharias DA. Palmitoyl acyltransferases, their substrates, and novel assays to connect them (Review). *Mol Membr Biol* 2009; **26**:14-31.

22 Ren J, Wen L, Gao X, Jin C, Xue Y, Yao X. CSS-Palm 2.0: an updated software for palmitoylation sites prediction. *Protein Eng Des Sel* 2008; **21**:639-644.

23 Abrami L, Leppla SH, van der Goot FG. Receptor palmitoylation and ubiquitination regulate anthrax toxin endocytosis. *J Cell Biol* 2006; **172**:309-320.

24 Xue Y, Chen H, Jin C, Sun Z, Yao X. NBA-Palm: prediction of palmitoylation site implemented in Naïve Bayes algorithm. *BMC Bioinformatics* 2006; **7**:458.

25 Sorek N, Yalovsky S. Analysis of protein S-acylation by gas chromatography-coupled mass spectrometry using purified proteins. *Nat Protoc* 2010; **5**:834-840.

26 Sorek N, Poraty L, Sternberg H, Bar E, Lewinsohn E, Yalovsky S. Activation status-coupled transient S acylation determines membrane partitioning of a plant Rho-related GTPase. *Mol Cell Biol* 2007; **27**:2144-2154.

27 Andreeva AV, Zheng H, Saint-Jore CM, Kutuzov MA, Evans DE, Hawes CR. Organization of transport from endoplasmic reticulum to Golgi in higher plants. *Biochem Soc Trans* 2000; **28**:505-512.

28 Brandizzi F, Frangne N, Marc-Martin S, Hawes C, Neuhaus JM, Paris N. The destination for single-pass membrane proteins is influenced markedly by the length of the hydrophobic domain. *Plant Cell* 2002; **14**:1077-1092.

29 Pandey GK, Cheong YH, Kim KN, *et al.* The calcium sensor calcineurin B-like 9 modulates abscisic acid sensitivity and biosynthesis in *Arabidopsis*. *Plant Cell* 2004; **16**:1912-1924.

30 Kolukisaoglu U, Weinl S, Blazevic D, Batistič O, Kudla J. Calcium sensors and their interacting protein kinases: genomics of the *Arabidopsis* and rice CBL-CIPK signaling networks. *Plant Physiol* 2004; **134**:43-58.

31 Kilian J, Whitehead D, Horak J, *et al*. The AtGenExpress global stress expression data set: protocols, evaluation and model data analysis of UV-B light, drought and cold stress responses. *Plant J* 2007; **50**:347-363.

32 D'Angelo C, Weinl S, Batistič O, *et al*. Alternative complex formation of the Ca-regulated protein kinase CIPK1 controls abscisic acid-dependent and independent stress responses in *Arabidopsis*. *Plant J* 2006; **48**:857-872.

33 Flannery AR, Czibener C, Andrews NW. Palmitoylation-dependent association with CD63 targets the Ca^{2+} sensor synaptotagmin VII to lysosomes. *J Cell Biol* 2010; **191**:599-613.

34 Bijlmakers MJ, Marsh M. The on-off story of protein palmitoylation. *Trends Cell Biol* 2003; **13**:32-42.

35 Robinson DG, Langhans M, Saint-Jore-Dupas C, Hawes C. BFA effects are tissue and not just plant specific. *Trends Plant Sci* 2008; **13**:405-408.

36 Emans N, Zimmermann S, Fischer R. Uptake of a fluorescent marker in plant cells is sensitive to brefeldin A and wortmannin. *Plant Cell* 2002; **14**:71-86.

37 Matsuoka K, Bassham DC, Raikhel NV, Nakamura K. Different sensitivity to wortmannin of two vacuolar sorting signals indicates the presence of distinct sorting machineries in tobacco cells. *J Cell Biol* 1995; **130**:1307-1318.

38 Greaves J, Salaun C, Fukata Y, Fukata M, Chamberlain LH. Palmitoylation and membrane interactions of the neuroprotective chaperone cysteine-string protein. *J Biol Chem* 2008; **283**:25014-25026.

39 Ohno Y, Kihara A, Sano T, Igarashi Y. Intracellular localization and tissue-specific distribution of human and yeast DHHC cysteine-rich domain-containing proteins. *Biochim Biophys Acta* 2006; **1761**:474-483.

40 Smotrys JE, Schoenfish MJ, Stutz MA, Linder ME. The vacuolar DHHC-CRD protein Pfa3p is a protein acyltransferase for Vac8p. *J Cell Biol* 2005; **170**:1091-1099.

41 Hou H, Subramanian K, LaGrassa TJ, *et al*. The DHHC protein Pfa3 affects vacuole-associated palmitoylation of the fusion factor Vac8. *Proc Natl Acad Sci USA* 2005; **102**:17366-17371.

42 Nadolski MJ, Linder ME. Molecular recognition of the palmitoylation substrate Vac8 by its palmitoyltransferase Pfa3. *J Biol Chem* 2009; **284**:17720-17730.

43 Heazlewood JL, Verboom RE, Tonti-Filippini J, Small I, Millar AH. SUBA: the Arabidopsis Subcellular Database. *Nucleic Acids Res* 2007; **35**:D213-D218.

44 Bartels DJ, Mitchell DA, Dong X, Deschenes RJ. Erf2, a novel gene product that affects the localization and palmitoylation of Ras2 in *Saccharomyces cerevisiae*. *Mol Cell Biol* 1999; **19**:6775-6787.

45 Hou H, John Peter AT, Meiringer C, Subramanian K, Ungermann C. Analysis of DHHC acyltransferases implies overlapping substrate specificity and a two-step reaction mechanism. *Traffic* 2009; **10**:1061-1073.

46 Sambrook J, Russel DW, eds. Molecular Cloning: A Laboratory Manual. Cold Spring Harbor, NY, USA: Cold Spring Harbor Laboratory Press, 2001.

47 Waadt R, Kudla J. *In Planta* visualization of protein interactions using bimolecular fluorescence complementation (BiFC). *CSH Protocols* 2008; 2008:pdb.prot4995. doi:10.1101/pdb.prot4995

48 Kim MJ, Baek K, Park CM. Optimization of conditions for transient *Agrobacterium*-mediated gene expression assays in *Arabidopsis*. *Plant Cell Rep* 2009; **28**:1159-1167.

(**Supplementary information** is linked to the online version of the paper on the *Cell Research* website.)